Techno-economic relevance of absorption chillers to enhance existing 3GDH

Boris Nérot, N Lamaison, Roland Bavière, Bruno Lacarrière, Mohamed Tahar Mabrouk

Available online at www.sciencedirect.com
ScienceDirect
Energy Reports 7 (2021) 282–293
www.elsevier.com/locate/egyr

17th International Symposium on District Heating and Cooling, DHC2020, 6–9th September 2021, Nottingham, England

Techno-economic relevance of absorption chillers to enhance existing 3GDH

B. Nérot[a,c], N. Lamaison[a], R. Bavière[b], B. Lacarrière[c,*], M.T. Mabrouk[c]

[a] Univ. Grenoble Alpes, CEA, Liten, Campus Ines, F-73375 Le Bourget du Lac, France
[b] Univ. Grenoble Alpes, CEA, Liten, DTCH, F-38000 Grenoble, France
[c] IMT Atlantique, Department of Energy Systems and Environment, GEPEA, F-44307, Nantes, France

Received 13 August 2021; accepted 22 August 2021

Abstract

This article studies the economical, technical and environmental aspects of a third generation district heating (DH) network with absorption chillers installed at substation level in order to satisfy the cooling demands. This network solution hence takes advantage of the distribution facilities of existing DH systems. The study aims at evaluating the technical and environmental performances of this new district heating architecture, when sized and operated according to an economic objective using the Mixed Integer Linear Programming (MILP) optimization formalism. It is compared to the case where cooling demands are met using individual chillers.

The paper first presents the production, distribution, demand and storage models. Regarding the demand side, different heating and cooling scenarios are studied by varying the proportions of residential and tertiary buildings. The model is fed in a second part with data from the French context. In particular, we rely on typical French weather conditions, thermal loads and energy costs.

The analysis of the results focuses on the cooling part. It appears that the thermal network solution achieves on average a 3.6% reduction in the levelized cost of space cooling energy. In the worst case space cooling exergy efficiency goes through a 82% decrease. GHG emissions decrease on average by 7.7% thanks to the absence of leakage of refrigerant with high global warming potential. Overall, these emissions are low due to the low carbon content of French electricity.

Peer-review under responsibility of the scientific committee of the 17th International Symposium on District Heating and Cooling, DHC2020, 2021.

Keywords: District heating; Transition; Space cooling; Absorption chiller; Mixed-integer linear programming; French context

* Corresponding author.
E-mail address: bruno.lacarriere@imt-atlantique.fr (B. Lacarrière).

https://doi.org/10.1016/j.egyr.2021.08.144

Peer-review under responsibility of the scientific committee of the 17th International Symposium on District Heating and Cooling, DHC2020, 2021.

Nomenclature

Variables

A	Thermal area (m^2)
$CAPEX$	Investment cost (€/W, €/m^3or €/m)
C_P	Specific heat capacity of water (J/(kg K))
d	Diameter (m)
dt	Time step (hours)
e	Plot ratio (–)
f_Q	HP COP parameter–compressor heat loss ratio (–)
E	Energy (J)
EX	Exergy (J)
H	Overall heat transfer coefficient (W/K)
L	Length (m)
m	Mass (kg)
n	Number
N	System lifetime (years)
$OPEX_F$	Fixed operation/maintenance cost (% $CAPEX$/yr)
$OPEX_V$	Variable operation/maintenance cost (€/MWh)
p	Proportion (%)
Q	Thermal energy (J)
r	Actualization rate (%)
S	Sign (–)
SE	Sizing variable (W, m^3 or m)
t	Hourly time step ([1, 8760])
T	Temperature (K)
U	Specific heat loss per routed meter of network trench (W/(K m))
V	Volume (m^3)
w	Effective width (m)
ΔP	HP COP parameter–pinch temperature (K)
ϵ	Storage losses (%/day)
$\eta_{is,c}$	HP COP parameter–compression efficiency (–)
η_P	Production efficiency (%)
ρ	Specific mass of water (kg/m^3)
ϕ	Heat gain (J)

Subscripts

a	Architecture (REF: reference, ABS: absorption)
D_k	Demand scenario
h	Node type (BU: buildings, CE: central)

1. Introduction

The International Energy Agency expects a threefold increase of worldwide space cooling demand for residential and tertiary sectors by 2050, compared to 2016 [1]. On the one hand, most of this demand involves countries with hot and humid climates whose interest for district cooling solutions is increasing but not yet generalized [2]. On the other hand, space cooling has less importance in regions where district heating (DH) networks are already used,

i	Building (1, 2, 3)
j	Demand (SH: space heating, DHW: domestic hot water, SC: space cooling)
x	Component (P: production, S: storage, N: network, C: carrier)
air, geo	Aerothermal, Geothermal
$elec, bio, gas$	Electricity, biomass, gas
int, sol	Internal, Solar
sys	Energy system

Superscripts

A	Relative to an area
IN, OUT	Incoming (import), Outcoming (export)
L	Relative to a length
T	Relative to a temperature

Acronyms

CC	Carbon content
CHP	Combined heat and power
COP	Coefficient of performance
DAC	Distributed absorption chillers
DC	Dry cooler
DH	District heating
EF	Emissions factor
EXF	Exergy factor
GHG	Greenhouse gases
GWP	Global warming potential
HP	Heat-pump
$LCOE$	Levelized cost of energy
$MILP$	Mixed-integer linear programming
MIP	Mixed-integer programming
SF	Simultaneity factor
WHS	Waste heat source

Operators

$\dot{.}$	Temporal derivative

such as Europe and part of Russia. In these regions, existing DH networks are mainly 2nd and 3rd generation systems with high operating temperatures leading to non-negligible distribution heat losses [3]. Because of DHW preparation and rather low building refurbishment rates [4,5], supply temperature is likely to remain in the 70–90 °C range in the coming years [6]. This temperature level is high enough to drive single-effect absorption chillers.

Following this idea, Chardon et al. [7] study three operating modes for an absorption chiller installed in a building substation. Among them, the cooling mode could provide cold to the building in summer. Regarding the cooling mode, Zhang et al. [8] further study an energy system consisting of a DH network with distributed absorption chillers (DAC) from a techno-economic point of view. The test case consists in single-effect absorption chillers driven by a DH network with supply and return temperatures being respectively 120 °C and 80 °C. Given the Chinese energy context consisting of coal combined heat and power (CHP) and power-only plants, they search for the minimum values of plant and absorption chiller efficiencies that allow achieving a positive fuel energy saving ratio. This ratio is calculated using a district cooling network fed by compression chillers as a reference case. Their results show that DAC are not economically competitive and does not provide energy savings for existing DH systems unless

their performances can improve significantly, for example using absorption dehumidifiers. Focusing on the Swedish case, Fahlén et al. [9] examine the strengths of a centralized trigeneration system. Their simulation of the Göteborg DH and district cooling systems shows that introducing centralized absorption chillers is economically competitive and CO_2 friendly as these machines – together with usual compression chillers – increase the utilization of CHP and excess heat. One strength of this work lies in the different shares of absorption chillers being considered to meet the city cooling needs, in replacement of compression chillers. Yet, the simulation considers only one set of thermal demand profiles which possibly leads to missing different operational modes of the system as the ratio of heating to cooling load varies.

In this article, a system consisting of a DH network that also drives DAC is compared to the case where DH is used only to deliver heat to the buildings and where cold demand is met using decentralized compression chillers, for different load scenarios. Section 2 describes the methodology and the model. In Section 3, the model is applied to the French case and the main results are analyzed, focusing on two extreme load scenarios. Section 4 concludes the work and underlines some limitations of the model.

2. Methodology

The model is here introduced in general terms. It covers both the technical and economic sides of the studied components. The model is based on the MILP formalism. While temperatures are parameters, energy flows (operation) and maximum capacities (sizing) are optimization variables (written in bold font).

A large part of the model is common to REF and ABS architectures. The following four aspects are described. First, sets of thermal demands are defined at the building and city scale. Then the decentralized equipment used in building, which depend on the architecture, are presented. The production and storage aspects of the central production plant are introduced the same way. Finally, the 3 GDH heat distribution network is described.

The model is then applied in the French context, the used data being tabulated along the description.

2.1. Thermal demand

Thermal demand is defined by assuming each building in the city can be classified as of a certain building type i. For each building type i, thermal demands are expressed as areal demands so that the demand at the city scale is obtained by multiplying the aggregated area of buildings of type i with this areal demand. This aggregation allows to consider only i time profiles for each thermal demand j, yet describing the city-scale energy system.

Three types of thermal demands j, namely space heating (SH), space cooling (SC) and domestic hot water (DHW), are considered in this study. These demands differ in (i) temperature levels ($T_{j,i}^{IN}$, $T_{j,i}^{OUT}$) and (ii) areal density $Q_{j,i}^{A} = Q_{j,i}/A_i$. Space heating and cooling demands definition follows the Tabula-Episcope project [10] and are shown in Eq. (1). Note that $\dot{Q}_{SH,i}^{A}(t) > 0$ (resp. $\dot{Q}_{SC,i}^{A}(t) > 0$) is possible only during the heating season (resp. cooling season), as defined in the Tabula-Episcope project.

$$\dot{Q}_{j,i}^{A}(t) = max\left(S \times \left(\frac{H_i\left(T_j - T_{air}(t)\right)}{A_i} - \left(\dot{\phi}_{int}^{A} + \dot{\phi}_{sol,j,i}^{A}\right)\right), 0\right) \text{ with } S = \begin{cases} 1\ if\ j = SH \\ -1\ if\ j = SC \end{cases} \quad (1)$$

$\dot{\phi}_{\mathrm{sol,j,i}}^{\mathrm{A}}$ derives from $Q_{sol,j,i}$ as tabulated in Tabula. It is constant in time, i.e. does not depend on the hour of the day, but is different for SH and SC and for each building i. $\dot{\phi}_{int}^{A}$ is constant all-year long and the same for all buildings.

Outdoor temperatures $T_{air}(t)$ come from a typical meteorological year (Grenoble, 2007–2016 period) [11] corrected according to the expected climate change variations by 2030 following the RCP4.5 IPCC scenario [12].

DHW demand is made of two parts and the same for all buildings. First, a constant demand accounts for thermal losses in the DHW circulation system of the building. It represents 40% of the annual DHW demand Q_{DHW}^{A} [13].

The remaining demand corresponds to draw-offs, and should account for simultaneity at the city scale. Braas et al. [13] show for single-family houses that the simultaneity factor in DHW draw-offs is much higher for a few living units (typically a building) than for around a hundred living units. As the district heating system considered in this study is made up of hundreds of living units, a conservative trade-off is chosen by selecting as a time profile an historical dataset measured for a group of 269 three rooms' apartments in Strasbourg, France [14].

Table 1. Building-specific properties defining the thermal demand.

Building i	A_i (m^2)	H_i (W K^{-1})	SH				SC			
			$\left(T^{IN}_{SH,i}, T^{OUT}_{SH,i}\right)$ (°C)	$\dot{\phi}^{A}_{sol,SH,i}$ (W m^{-2})	$Q^{A}_{SH,i}$ ($kWh.m^{-2}yr^{-1}$)	$\dot{Q}^{A,max}_{SH,i}$ (kW m^{-2})	$\left(T^{IN}_{SC,i}, T^{OUT}_{SC,i}\right)$ (°C)	$\dot{\phi}^{A}_{sol,SC,i}$ (W m^{-2})	$Q^{A}_{SC,i}$ (kWh m^{-2} yr^{-1})	$\dot{Q}^{A,max}_{SC,i}$ (kW m^{-2})
1	460	1481	(60, 35)	5.10	141	0.085	–	–	–	–
2	539	564	(35, 25)	2.91	32	0.025	(10, 15)	5.37	13.5	0.017
3	460	1481	(50, 35)	5.10	141	0.085	(7, 12)	11.7	18.7	0.040

Table 2. Properties defining the thermal demand (common to all building types).

$\dot{\phi}^{A}_{int}$ (W m^{-2})	Q^{A}_{DHW} (kWh m^{-2} yr^{-1})	$\left(T^{IN}_{DHW,i}, T^{OUT}_{DHW,i}\right)$ (°C)	T_{SH} (°C)	T_{SC} (°C)
3	20	(70, 40)	20	26

For the present analysis, three types of buildings are considered, i.e. two residential and one tertiary. Tables 1 and 2 summarize all the thermal demand parameters for these buildings.

Twenty-one demand scenarios D_k are then defined by varying the proportion of each building p_i in the system total thermal area A_{BU} (Eq. (2)) so that $p_i \in \{0, 20, 40, 60, 80, 100\}$ and $\sum_i p_i = 100$.

$$A_{i,D_k} = \frac{p_i}{100} A_{BU} \tag{2}$$

2.2. Substation

The study considers two architectures that suppose the existence of SH and SC distribution systems at the building level. These architectures, shown in Fig. 1, are the following:

(i) Reference (REF) in which SH and DHW demands are satisfied using the DH network while SC demand is met using compression air-cooled chillers at the building level.
(ii) Absorption (ABS) where substations are equipped with absorption chillers driven by the DH network to meet SC needs.

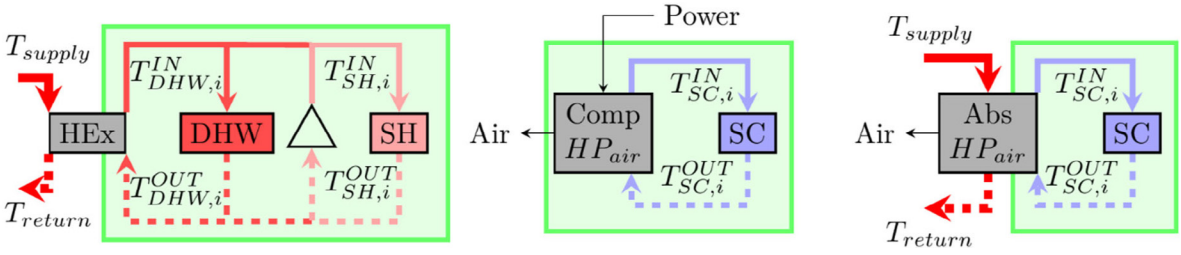

Fig. 1. Substation layout of buildings. Heating system (left, common to both architectures), cooling system for REF architecture (middle), cooling system for ABS architecture (right).

The heat exchanger HEx is common to REF and ABS and hence not detailed. The properties of absorption and compression chillers are given in Table 3. Each of these aerothermal chillers comes with a dry cooler component DC that moves the condenser heat to the outdoor air. Its electricity consumption is set to 2.75% of the dissipated heat, which is a figure observed on a set of commercially available machines (the same source is used for the $CAPEX_P$ of DC). The electricity consumption of the absorption chiller (solution pump) is considered to be 2.6% of the cold production [15].

The GHG emissions due to refrigerant leakage of comp-HP_{air} are accounted for. A 4% annual and 15% end-of-life leakage shares are considered [19]. A linear regression on a dataset of six air-cooled HP of small capacity yields a 0.3 kg/kW specific charge of refrigerant ($R^2 = 0.895$). R32 refrigerant which has a GWP of 677 over 100 years [20] is used to comply with the European Union HFC phase-down [21].

Table 3. Properties of production equipment in substation.

Production	η_P (%)	$CAPEX_P$ (€ kW^{-1})	$OPEX_{F,P}$ (%$CAPEX$ yr^{-1})	$OPEX_{V,P}$ (€ MWh^{-1})	N_P (yr)
Abs-HP$_{air}$ [16]	170%	1458	0.36	1	25
Comp-HP$_{air}$ [17]	[18] ($\Delta P = (3, 7)$ K, $\eta_{is,c} = 0.75$ et $f_Q = 0.2$)	940	2.96	0	18
DC	–	128.4	0	0	Same than HP$_{air}$

2.3. Distribution network

The distribution network, whose parameters are listed in Table 4, carries heat from a central production plant to the buildings. It is worth mentioning here that the distribution network is the same for both architectures for a given demand scenario: in ABS architecture, the peak mass flow rate still occurs for SH satisfaction and thus unchanged compared to REF. Hence, the transition from REF to ABS is legitimate. The investment and fixed operation and maintenance costs that are common to both architectures are not accounted for but a variable operating cost is. The thermal losses are taken into account through U and $T_{soil}(t)$.

Table 4. Properties of distribution network.

$L_{network}$ (km)	U (W K^{-1} m^{-1})	A_{BU} (km^2)	(T_{supply}, T_{return}) (°C)	T_{soil} (t) (°C)	$OPEX_{V,N}$ (€ MWh^{-1})	N_N (yr)
170 City of Grenoble (FR)	0.7 [22,23]	5.1 [24,25] with $e = 0.5$	(90 , 60)	2 m depth [26]	1.5 [27]	40 [28]

2.4. Central production plant

Six production units are available at the central production plant (Table 5). They are of four kinds:

- Cogeneration of extraction-condensing type powered by biomass or natural gas.
  Their electricity production is either consumed locally or sold to the grid at a feed-in tariff equal to the buying one.
  For ABS architecture, it can also be used by buildings to operate Abs-HP$_{air}$, since both centralized production and decentralized Abs-HP$_{air}$ are operated by the same entity, i.e. the DH operator. This exchange is unconstrained in capacity and energy and done at no costs.
- Boilers powered by electricity or natural gas.
- Heat pump using geothermal energy at temperature T_{geo}.
- Waste heat, recovered using a heat exchanger. The recovery can be partial only as no binding contract between the heat producer and the DH system is modeled. In reality, the need of a reliable solution to get rid of excess heat is real for some industries.

Table 5. Properties of production equipment at the central production plant.

Production	η_P (%)	$CAPEX_P$ (€ kW^{-1})	$OPEX_{F,P}$ (%$CAPEX$ yr^{-1})	$OPEX_{V,P}$ (€ MWh^{-1})	N_P (yr)
Bio-CHP ([29], wood pellets)	[29]	2000	2.85	2	40
Gas-CHP ([29], combined cycle)	[29]	900	3.33	4.5	25
Comp-HP$_{geo}$ [16] ($T_{geo} = 12$ °C)	[18] ($\Delta P = 3$ K, $\eta_{is,c} = 0.75$ et $f_Q = 0.2$)	670	0.3	1.7	25
Elec-Boil (adapt. [16])	99%	128	0.71	0.9	20
Gas-Boil [16]	97.8% (adapt [30])	60	3.25	1.1	25
WHS-HEx [27]	95%	100	0	1.5	40

These equipment rely on electricity, natural gas, biomass and waste heat. These vectors are bought from the grid and associated with CO_2 emissions (Table 6).

Table 6. Properties of energy carriers (lower calorific value).

Carrier	$\boldsymbol{EF}$ (kgEqCO_2 kWh^{-1})	Availability	Energy flow direction	$\boldsymbol{OPEX_{V,C}}$ (€ MWh^{-1})		
				Central production plant	$i = 2$	$i = 3$
Electricity	France, 2019 [31] (mean: 0.054, std: 0.021)	–	Import, Export (CHP)	SPOT, France, 2019 [31] (mean: 38, std: 16)	189.9 [32]	125.6 [32]
Gas	0.227 [33]	–	Import	40 [32]	–	–
Biomass	0.0304 [33]	Energy limit: $0.164 \sum_{i,j} Q_{i,j,D_k}$ (national values, [34])	Import	25 [29]	–	–
$\boldsymbol{WHS}$	*0*	Capacity limit: 16 MW	Import	10 [35]	–	–

Available storage equipment at the central production plant are listed in Table 7. Two storage units are implemented:

- A short-term tank storage, which is charged and discharged directly and use the network heat media.
- A long-term pit storage. In addition to a daily power loss, thermal losses are taken into account by defining storage temperatures lower than the network temperatures. Hence, it is charged using a heat exchanger but a heat pump is needed for discharge. Their properties are the same as WHS-HEx and Comp-HP_{geo}, respectively.

The storage (S) operation and sizing constraints are given in Eqs. (3), (4) and (5), with $\mathbf{n_S}$ the optimized number of storage units (integer variable).

$$\boldsymbol{Q_S}(\boldsymbol{t}+\mathbf{1}) = (1-\epsilon)^{\frac{1}{24}} \times \boldsymbol{Q_S}(\boldsymbol{t}) + \left(\dot{\boldsymbol{Q}}_{\boldsymbol{S}}^{\boldsymbol{IN}}(\boldsymbol{t}) - \dot{\boldsymbol{Q}}_{\boldsymbol{S}}^{\boldsymbol{OUT}}(\boldsymbol{t})\right) \times dt \tag{3}$$

$$0 \leq \boldsymbol{Q_S}(\boldsymbol{t}) \leq \rho C_P \left(T_S^{IN} - T_S^{OUT}\right) \times \boldsymbol{SE_S} \tag{4}$$

$$\boldsymbol{SE_S} = V \times \boldsymbol{n_s} \tag{5}$$

Table 7. Properties of storage equipment .
Source: Adapted from [36].

Storage	ϵ_S (% day^{-1})	Temperatures (°C)	V_S (m^3)	n_S^{max}	Charge/ Discharge	Max power (MW)	$CAPEX_S$ (€ m^{-3})	$OPEX_{F,S}$ (%$CAPEX$ yr^{-1})	N_S (yr)
Short-term	2	(T_{supply}, T_{return})	3000	3	Direct	1.74	173	0.29	40
Long-term	0.2	(70, 35)	70 000	1	HEx/Comp HP	30	37.3	0.52	20

2.5. Objective function

The optimization is carried out at an hourly time step over a one-year time span. The objective function to be minimized is the levelized cost of energy (LCOE). All costs (energy carriers, production and storage equipment, distribution network) are annualized using $N_{sys} = 40$ years and $r = 3.5\%$ [37]. Production and storage equipment x have a sizing variable $\boldsymbol{SE_{a,D_k,x}}$. Production equipment, distribution network and energy carriers have an annual energy variable $\boldsymbol{E_{a,D_k,x}}$ (production, import/export).

Eq. (6) defines the objective function $\boldsymbol{LCOE_{a,D_k}}$ as a sum of contributions of element x.

$$\boldsymbol{LCOE_{a,D_k}} = \frac{\sum_x \sum_{y=1}^{N_{sys}} \left[CAPEX_x \left(rep_x(y) + OPEX_{F,x}\right) \times \boldsymbol{SE_{a,D_k,x}} + OPEX_{V,x} \times \boldsymbol{E_{a,D_k,x}}\right](1+r)^{-y}}{\sum_{i,j} Q_{i,j,D_k} \sum_{y=1}^{N_{sys}} (1+r)^{-y}} \tag{6}$$

With $rep_x\,(y) = 0$ if $y-1$ is not a multiple of N_x and given by Eq. (7) in the opposite case.

$$rep_x\,(y) = 1\ if\ N_{sys} - (y-1) \geq N_x, else \frac{N_{sys} - (y-1)}{N_x} \tag{7}$$

2.6. Indicators

Four indicators are defined to assess the performances of the ABS and REF architectures for each demand scenario:

- Net quantity of electricity consumed per unit of final thermal energy $I_{elec,a,D_k}(\%)$ (Eqs. (8) and (9));

$$\mathrm{I_{elec,a,D_k}} = \frac{\sum_{\mathbf{h}} \mathbf{E^{IN}_{elec,h,a,D_k}} - \mathbf{E^{OUT}_{elec,CE,a,D_k}}}{\sum_{\mathrm{j}} \sum_{\mathrm{i}} \mathrm{Q_{j,i,D_k}}} \tag{8}$$

- Exergy efficiency regarding final thermal energy $I_{EX,a,D_k}(\%)$ (Eq. (9), using $\mathrm{T_0} = 25\ ^\circ\mathrm{C}$);

$$\mathrm{I_{EX,a,D_k}} = \frac{\sum_{\mathrm{j}} \sum_{\mathrm{i}} \pm \mathrm{Q_{j,i,D_k}} \left(1 - \frac{\mathrm{T_0}}{\mathrm{T^{OUT}_{j,i}} - \mathrm{T^{IN}_{j,i}}} \ln\left(\frac{\mathrm{T^{OUT}_{j,i}}}{\mathrm{T^{IN}_{j,i}}}\right)\right)}{\mathbf{Q_{WHS,CE,a,D_k}} \left(1 - \frac{\mathrm{T_0}}{\mathrm{T^{OUT}_{WHS}} - \mathrm{T^{IN}_{WHS}}} \ln\left(\frac{\mathrm{T^{OUT}_{WHS}}}{\mathrm{T^{IN}_{WHS}}}\right)\right) + \mathbf{E^{IN}_{bio,CE,a,D_k}} + \mathbf{E^{IN}_{gas,CE,a,D_k}} + \sum_{\mathbf{h}} \mathbf{E^{IN}_{elec,h,a,D_k}} - \mathbf{E^{OUT}_{elec,CE,a,D_k}}} \tag{9}$$

- Carbon content of final thermal energy $I_{CC,\mathrm{a},D_k}(\mathrm{kgEqCO_2/MWh})$;
- Levelized cost of final thermal energy $\boldsymbol{LCOE_{a,D_k}}(€/\mathrm{MWh})$;

These indicators are calculated for the cold production only as the focus in this study is on SC demand. This is straightforward for REF architecture as heating (SH, DHW) and SC demands are satisfied independently.

For ABS architecture, these indicators values are the same than for REF for the heating part. The cooling part is obtained as the difference between the all-demands part and the heating part.

3. Results and discussion

The output of the model when applied on the French case are presented hereafter. The values of the four indicators introduced in Chapter 2 and their analysis are presented and commented. The results are then studied more in detail for two particular demand scenarios.

Fig. 2 presents each indicator for each demand scenario. Each box is a demand scenario defined by the proportions (p_1, p_2, p_3) of buildings, with p_2 on the x-axis, p_3 on the y-axis and p_1 read diagonally and verifying $p_1 = 100 - p_2 - p_3$. The value annotated in each box is for REF architecture while a color scale shows the relative variation using ABS architecture (see Eq. (10)).

$$VAR\left(I_{D_k}\right) = 100 \times \frac{I_{ABS,D_k} - I_{IC,D_k}}{I_{IC,D_k}} \tag{10}$$

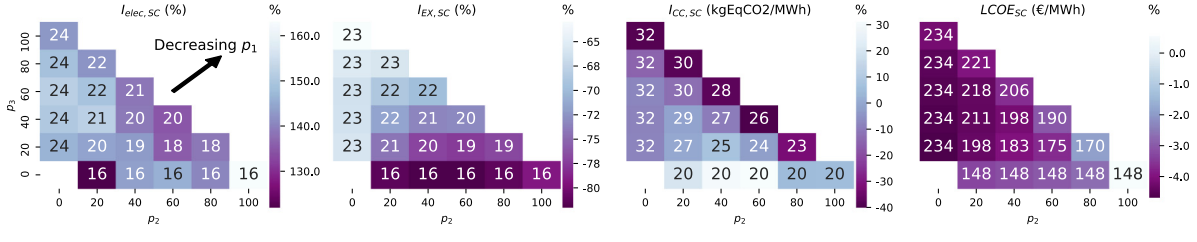

Fig. 2. Indicators values for REF architecture (annotation) and variation of indicators from REF to ABS architecture (color scale).

For example, the carbon content $I_{CC,SC}$, which is equal to 29% for the demand scenario (40%, 20%, 40%) decreases by approximately 1% when transitioning from REF to ABS architecture.

For REF architecture, the electricity content of the SC load $I_{elec,SC}$ is nearly equal to the opposite of the mean annual COP of Comp-HP$_{\text{air}}$ (the former is the ratio of mean annual energies (Eq. (8)) while the latter is an annual mean of energy ratios). Surprisingly, this electricity dependence increases in ABS architecture. On the one hand, the central thermal power production driving the building level Abs-HP$_{\text{air}}$ depends on gas, waste heat and biomass in addition to the sole electric vector. On the other hand, the COP of Abs-HP$_{\text{air}}$ is lower than the one of Comp-HP$_{\text{air}}$ leading to an increased drive energy. Overall, the second effect compensates the first since, on average in ABS architecture, 36% only of the energy consumed to satisfy the SC demand is not electricity (0% for REF architecture, not seen on Fig. 2).

Exergy efficiency $I_{EX,SC}$ in REF architecture is lower for high p_2 than for high p_3. Indeed, low SC temperatures of building 2 allow its Comp-HP$_{\text{air}}$ to run at high COP, yet not high enough to counterbalance the low load exergy associated with SC demand. When transitioning from REF to ABS, the chiller lower COP leads to an exergy efficiency decrease. It is all the more noticeable that Comp-HP$_{\text{air}}$ has a good COP, i.e. for high p_2.

On average, 63% of the eq.CO2 content of final energy $I_{CC,SC}$ in REF architecture is due to refrigerant leakage at the building level, the rest being energy related emissions. This refrigerant part is proportional to the ratio $\dot{Q}_{SC}^{A,max}/Q_{SC}^{A}$, which is 37% smaller in building 2 compared to building 3. Consequently, a gain in GHG emissions is observed for high p_3 when considering ABS architecture for which no refrigerant leakage takes place. Yet, energy related emissions increase on average by a factor 2.4 from REF to ABS.

The high $LCOE_{SC}$ in REF architecture depends again on the ratio $Q_{SC}^{A,max}/Q_{SC}^{A}$, as a large $Q_{SC}^{A,max}$ leads to high $CAPEX$ and $OPEX_F$ of Comp-HP$_{\text{air}}$: this equipment part accounts for 85% of $LCOE_{SC,REF}$ on average, the remaining 15% being the cost of electricity. The transition to ABS architecture is beneficial to the $LCOE$: though the $CAPEX$ of ABS-HP$_{\text{air}}$ is 55% higher than the one of Comp-HP$_{\text{air}}$, its lower $OPEX_F$ and longer equipment lifetime (Table 3) lead to a lower annualized cost. The variable cost of distribution $OPEX_V$ is only 2.14€/MWh for SC in ABS architecture.

Regarding the storage facilities, the maximum number of short-term tanks (3) are chosen in every scenario. Long-term storage is never used since it presents a prohibitive cost for a small value-added as there is no seasonal heat production to shift.

The focus is now on both heating and cooling aspects of the 2 extreme scenarios $p_2 = 100\%$ and $p_3 = 100\%$. For these scenarios, the sizing of production equipment in central production plant is shown in Fig. 3 (note that for CHP units, the reference production is electricity). In both architectures, a base production in central plant is ensured by equipment with low operating costs (Comp-HP$_{\text{geo}}$, WHS-HEx) while low-CAPEX equipment cover the

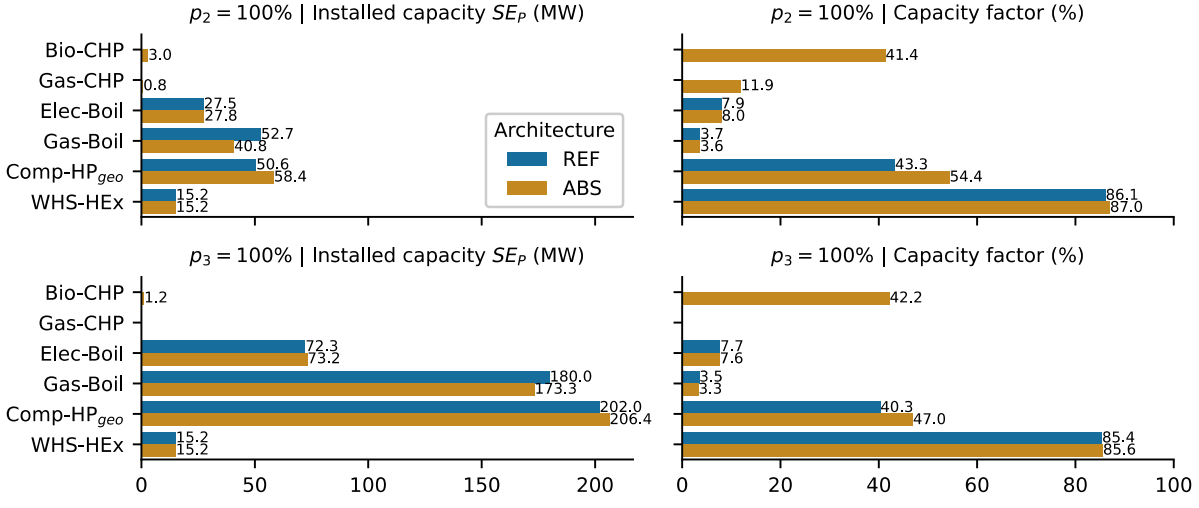

Fig. 3. Installed capacity SE_P (MW) (left) and capacity factor (%) (right) for scenarios $p_2 = 100\%$ (top) and $p_3 = 100\%$ (bottom).

peak demands (Elec-Boil, Gas-Boil). WHS-HEx is not used all year round since the periods of low-cost electricity are beneficial to Comp-HP_{geo} operation.

Very small CHP capacities are used in ABS architecture in order to provide the buildings with cheap electricity. This electricity covers 18% of the annual chiller needs for $p_3 = 100\%$ but 84% for $p_2 = 100\%$, the remaining part being bought from the grid at high cost (Table 6). The more interesting electricity cost of building 3 leads to a smaller sizing of CHP units for $p_3 = 100\%$. Overall, using electricity from CHP units to run Comp-HP_{geo} is not economically interesting, as the cost of electricity bought from the grid in central production plant is low and can be anticipated.

The transition from REF to ABS architecture leads to an increase of the annual heat production in central plant of 28.7% and 14.6% for demand scenarios $p_2 = 100\%$ and $p_3 = 100\%$. Each of these values are in the order of magnitude of the ratio $Q^A_{SC,i}/(Q^A_{DHW,i} + Q^A_{SH,i})$. Yet, two opposite effects are to be accounted for. Firstly, Abs-HP, whose COP is lower than one, leads to an increase of the load seen by the network compared to the real SC load. Secondly, distribution losses are lower in SC season than in SH season because of the soil temperature being higher.

Similarly, the higher utilization rate of the distribution network in ABS compared to REF architecture leads to a 9.7% decrease in relative distribution losses on average.

Fig. 3 and Table 8 reveal the substitution of a small part of Gas-Boil production by Comp-HP_{geo} and Bio-CHP in ABS architecture. Indeed, as the use of electricity production by buildings during the SC season makes the investment in Bio-CHP attractive, this unit – which fuel is cheaper than gas – can run all year long to produce heat.

Table 8. Evolution of energy consumption in the system (first four columns) and heat production at central plant (last column) from REF to ABS architecture for scenarios $p_2 = 100\%$ and $p_3 = 100\%$.

	Electricity	Biomass	Gas	WHS	Annual centralized heat production
$p_2 = 100\%$	+15%	–	−14%	+1.0%	+28.7%
$p_3 = 100\%$	+9.4%	–	−8.0%	+0.2%	+14.6%

4. Conclusion and outlook

In this article, a reference 3 GDH architecture with individual cooling solutions (REF) was compared with the same system providing cooling using absorption HPs at substation level (ABS), for different types of thermal demands, using a near-LP model. It was shown that despite achieving lower exergy efficiency, ABS architecture also leads to lower distribution losses, higher capacity factors of production equipment in central plant, lower GHG emissions and lower LCOE. The main limitations of the model are the following: (i) the absorption chiller COP is the same whatever the temperature at the evaporator and condenser sides, (ii) the lack of operational constraints allows unrealistic use of production equipment, (iii) the electricity cost is assumed to be perfectly anticipated, and (iv) the excess heat does not come with an associated emissions factor. Moreover, the assessment of electrical grid reinforcement cost might be needed. A regression from Gupta et al. [38] based on the electrical installed chiller capacity and applied on the current model shows that the grid reinforcement would represent on average a 41% extra cost compared to current cooling LCOE, with few variations between REF and ABS architecture due to an important constant part.

Regarding the perspectives, the assessment of which heating and cooling technologies are best suitable in a given physical and economic context should be done considering 4th and 5th generation district heating and cooling, as these architecture significantly differ from ABS architecture in the way heat and cold are produced and delivered.

Declaration of competing interest

The authors declare that they have no known competing financial interests or personal relationships that could have appeared to influence the work reported in this paper.

Acknowledgment

We gratefully acknowledge ADEME (French Environment and Energy Management Agency) for their financial contribution in funding the PhD thesis of Boris Nérot.

References

[1] The future of cooling, IEA, Paris. 2018, [Online]. Available: https://www.iea.org/reports/the-future-of-cooling.

[2] Eveloy V, Ayou D. Sustainable district cooling systems: Status, challenges, and future opportunities, with emphasis on cooling-dominated regions. Energies 2019;12(2):235. http://dx.doi.org/10.3390/en12020235.

[3] Werner S. International review of district heating and cooling. Energy 2017;137:617–31. http://dx.doi.org/10.1016/j.energy.2017.04.045.

[4] Volkova A, Mašatin V, Siirde A. Methodology for evaluating the transition process dynamics towards 4th generation district heating networks. Energy 2018;150:253–61. http://dx.doi.org/10.1016/j.energy.2018.02.123.

[5] Jangsten M, Kensby J, Dalenbäck J-O, Trüschel A. Survey of radiator temperatures in buildings supplied by district heating. Energy 2017;137:292–301. http://dx.doi.org/10.1016/j.energy.2017.07.017.

[6] Deng J, Wang RZ, Han GY. A review of thermally activated cooling technologies for combined cooling, heating and power systems. Prog Energy Combust Sci 2011;37(2):172–203. http://dx.doi.org/10.1016/j.pecs.2010.05.003.

[7] Chardon G, Le Pierrès N, Ramousse J. On the opportunity to integrate absorption heat pumps in substations of district energy networks. Thermal Sci Eng Progr 2020;20:100666. http://dx.doi.org/10.1016/j.tsep.2020.100666.

[8] Zhang Q, Wang Y, Zhang X, Wang M, Wang G. Techno-economic analysis of distributed absorption cooling system driven by a district heating system. Energy Efficiency 2020;13(8):1689–703. http://dx.doi.org/10.1007/s12053-020-09903-2.

[9] Fahlén E, Trygg L, Ahlgren EO. Assessment of absorption cooling as a district heating system strategy – A case study. Energy Convers Manage 2012;60:115–24. http://dx.doi.org/10.1016/j.enconman.2012.02.009.

[10] Loga T, Stein B, Diefenbach N. Tabula building typologies in 20 European countries—Making energy-related features of residential building stocks comparable. Energy Build 2016;132:4–12. http://dx.doi.org/10.1016/j.enbuild.2016.06.094.

[11] Photovoltaic geographical information system. 2020, https://re.jrc.ec.europa.eu/pvg_tools/fr/tools.html (accessed Jun. 05, 2020).

[12] Drias, les futurs du climat - accueil. 2021, http://drias.meteo.fr/ (accessed Feb. 21, 2021).

[13] Braas H, Jordan U, Best I, Orozaliev J, Vajen K. District heating load profiles for domestic hot water preparation with realistic simultaneity using DHWcalc and TRNSYS. Energy 2020;201:117552. http://dx.doi.org/10.1016/j.energy.2020.117552.

[14] Les Besoins D'eau Chaude Sanitaire En Habitat Individuel Et Collectif. ADEME; 2016.

[15] Triché D. Étude numérique et expérimentale des transferts couplés de masse et de chaleur dans l'absorbeur d'une machine à absorption ammoniac-eau (These de doctorat), Université Grenoble Alpes (ComUE); 2016, Accessed: Jun. 23, 2021. [Online]. Available: https://www.theses.fr/2016GREAI095.

[16] Generation of electricity and district heating, danish energy agency. 2020, Accessed: Nov. 28, 2020. [Online]. Available: https://ens.dk/en/our-services/projections-and-models/technology-data/technology-data-generation-electricity-and.

[17] Heating installations, danish energy agency. 2018, Accessed: Dec. 07, 2020. [Online]. Available: https://ens.dk/en/our-services/projections-and-models/technology-data/technology-data-individual-heating-plants.

[18] Jensen KJ, Ommen T, Reinholdt L, et al. Heat Pump COP, Part 2: Generalized COP Estimation of Heat Pump Processes. International Institute of Refrigeration (IIR); 2018, http://dx.doi.org/10.18462/IIR.GL.2018.1386.

[19] Hwang Y. Heat pump systems with low GWP refrigerants, In 13th IEA Heat Pump Conference, Korea: 2021; [Online]. Available: https://heatpumpingtechnologies.org/annex54/wp-content/uploads/sites/63/2021/05/1-annex54workshopieahpcoperatinagent.pdf.

[20] Myhre G, et al. Chapter 8 AR5, IPCC, Anthropogenic and Natural Radiative Forcing 5.

[21] Pardo P, Mondot M. Experimental evaluation of R410a, R407c and R134a alternative refrigerants in residential heat pumps. 2021, [Online]. Available: https://heatpumpingtechnologies.org/annex54/wp-content/uploads/sites/63/2021/05/2-annex54workshopieahpcpierrepardocetiat.pdf.

[22] Masatin V, Latõšev E, Volkova A. Evaluation factor for district heating network heat loss with respect to network geometry. Energy Procedia 2016;95:279–85. http://dx.doi.org/10.1016/j.egypro.2016.09.069.

[23] Handbook of planning of district heating networks, Working Committee QM District Heating, Switzerland: Aug. 2020; [Online]. Available: http://www.verenum.ch/index_QMDH.html.

[24] Persson U, Werner S. Heat distribution and the future competitiveness of district heating. Appl Energy 2011;88(3):568–76. http://dx.doi.org/10.1016/j.apenergy.2010.09.020.

[25] Persson U, Wiechers E, Möller B, Werner S. Heat roadmap europe: Heat distribution costs. Energy 2019;176:604–22. http://dx.doi.org/10.1016/j.energy.2019.03.189.

[26] Kusuda T, Achenbach PR. Earth temperature and thermal diffusivity at selected stations in the United States. 1965, p. 236.

[27] Energy transport, danish energy agency. 2020, Accessed: Nov. 28, 2020. [Online]. Available: https://ens.dk/en/our-services/projections-and-models/technology-data/technology-catalogue-transport-energy-co2.

[28] Leurent M. Cost–benefit analysis of district heating systems using heat from nuclear plants in seven European countries. 2018, p. 19.

[29] Dahl M, Brun A, Andresen GB. Cost sensitivity of optimal sector-coupled district heating production systems. Energy 2019;166:624–36. http://dx.doi.org/10.1016/j.energy.2018.10.044.

[30] Chaudières à condensation, Energie Plus Le Site. 2020, https://energieplus-lesite.be/techniques/chauffage10/chauffage-a-eau-chaude/chaudieres-a-condensation/ (accessed Jun. 11, 2020).

[31] Transparency platform restful API - user guide. 2021, https://transparency.entsoe.eu/content/static_content/Static%20content/web%20api/Guide.html (accessed Feb. 22, 2021).

[32] Base de données - Eurostat. 2020, https://ec.europa.eu/eurostat/fr/data/database (accessed Dec. 01, 2020).

[33] Ademe - site bilans GES. 2020, https://www.bilans-ges.ademe.fr/ (accessed May 25, 2020).

[34] IEA – international energy agency, IEA. 2021, https://www.iea.org (accessed Jan. 21, 2021).

[35] Home - flexynets. 2020, http://www.flexynets.eu/en/ (accessed Jul. 07, 2020).

[36] Energy storage, danish energy agency. 2020, Accessed: Jan. 14, 2021. [Online]. Available: https://ens.dk/en/our-services/projections-and-models/technology-data/technology-data-energy-storage.
[37] Carpenè L, Haeusler L. Réseaux de Chaleur Et de Froid, état Des Lieux de la Filière: Marchés, Emplois, Coûts. ADEME; 2019.
[38] Gupta others R. Spatial analysis of distribution grid capacity and costs to enable massive deployment of PV, electric mobility and electric heating. Appl Energy 2021;287:116504. http://dx.doi.org/10.1016/j.apenergy.2021.116504.